Nonlinear Distortion Cancellation Using LINC Transmitters in OFDM Systems

Paloma García, Alfonso Ortega, Jesús de Mingo, *Member, IEEE*, and Antonio Valdovinos, *Member, IEEE*

***Abstract*—The *LI*near amplification using *N*onlinear *C*omponents (LINC) technique is a well-known power amplifier linearization method to reduce out-of-band interferences in a nonconstant envelope modulation system, such as Digital Video Broadcasting (DVB) system, which is based on a very sensitive to nonlinear distortions OFDM modulation scheme. The major drawback of LINC transmitters is the inherited sensitivity to gain and phase imbalances between the two amplifier branches. In this paper, a novel full-digital base band method, which corrects any gain and phase imbalances in LINC transmitters mainly due to the un-matching of the two amplifier paths, is described. Amplifiers are characterized by a level-dependent complex gain using a memoryless model. The method uses adaptive signal processing techniques to obtain the optimal complex coefficients to correct gain and phase imbalances. Its main advantage is the ability to track the input signal variations and adapt to the changes of amplifier nonlinear characteristics. Other effects are included in the analysis such as quadrature modulator and demodulator impairments. A computer simulation has been carried out to verify method functionality.**

***Index Terms*—Adaptive system, amplifier linearization, nonlinear distortion, ortogonal frequency-division multiplexing (OFDM).**

I. Introduction

THE NEW digital audio broadcasting (DAB) and digital video broadcasting-terrestrial (DVB-T) are emergent telecommunication systems that are based on a multicarrier modulation as the OFDM schemes (Orthogonal Frequency Division Multiplexing). An OFDM signal consists of a sum of subcarriers that are modulated by using phase shift keying (PSK) or quadrature amplitude modulation (QAM) [1]. The OFDM transmission is an efficient way to deal with multipath and its implementation is less complex than an equalizer. It is also robust against narrowband interferences, because such interferences affect only a small percentage of the subcarriers. Another advantage of the OFDM system is that the digital transmitter and receiver can be efficiently implemented using the Fast Fourier Transform (FFT) algorithm. However, one of its drawbacks is its sensitivity to nonlinear distortions due to its greatly variable envelope and high peak to mean envelope power ratio values [2]–[4]. As a result of nonlinearity effects (mainly from power amplifier), the transmission spectrum is expanded into adjacent channels, an effect known as ACI (Adjacent Channel Interference). One way to achieve linear amplification is by using a class A power amplifier working with a high backoff, which corresponds to moving the operating point of the amplifier to the linear region. However, it implies low power efficiency. High power efficiency can be obtained with class AB power amplifiers, but they show more nonlinear characteristics. In order to achieve both spectrum and power efficiency, several classical linearizing techniques for power amplifiers have been proposed in the technical literature. These techniques are usually categorized as Feed-forward, Feedback, Predistortion and LINC transmitter. According to the recent literature [5]–[8], [17], the predistortion technique has been the more useful scheme in order to reduce the effects of nonlinear distortion on the performance of OFDM systems. In this paper the authors have proposed and analyzed an adaptive digital LINC transmitter structure. LINC is an acronym for linear amplification with nonlinear components. A schematic diagram of a LINC transmitter is depicted in Fig. 1. Its major drawback is the inherited sensitivity to gain and phase imbalances between the two amplifier branches [9], [10]. Several authors have considered different methods to correct the imbalances in LINC transmitters [11]–[14], but the novel method presented here uses adaptive signal processing techniques. It is carried out in base-band and is full-digital.

Manuscript received December 10, 2003; revised May 10, 2004. This work was supported by the CICYT (Spain) under grant TIC2001-2481 and TEC2004–04529.

P. García and A. Valdovinos are with Centro Politécnico Superior, University of Zaragoza, Spain.

A. Ortega is with the Communications Technologies Group (UZ) and the Aragon Institute of Engineering Research (I3A).

J. de Mingo is with the Departamento de Ingeniería Electrónica y Comunicaciones, Universidad de Zaragoza.

Digital Object Identifier 10.1109/TBC.2004.842527

II. LINC Transmitter

One of the reasons that the LINC transmitter has not been widely used, is the difficulty to achieve the accurate gain and phase matching required between the two paths. Errors in gain and/or phase matching will cause incomplete cancellation of unwanted elements in wideband phase modulated signals. As a result, a large number of unwanted spurious products appear in the output spectrum, as observed previously [9], [10], [12], [15].

The effect of gain and phase imbalances between the two paths may be analyzed as follows. The source signal may be written in complex general format as [15], [20]

$$s(t) = c(t)\, e^{j\rho(t)} \qquad 0 < c(t) \le c_{\max}. \tag{1}$$

The source signal is separated into two constant-envelope signals by a Signal Component Separator (SCS) as shown in Fig. 1. These signals are calculated as

$$\begin{aligned} s_1(t) &= \frac{s(t)}{2}\left[1 - e_s(t)\right] \\ s_2(t) &= \frac{s(t)}{2}\left[1 + e_s(t)\right]. \end{aligned} \tag{2}$$

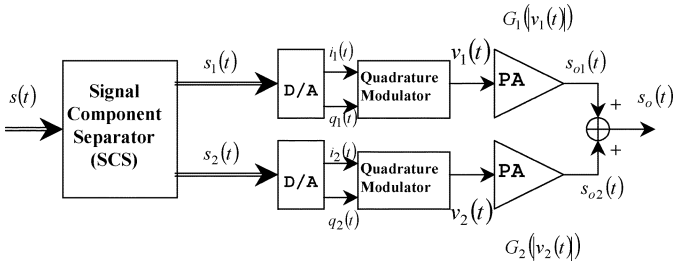

Fig. 1. Schematic diagram of the LINC transmitter.

Where $e_s(t)$ is a signal that is in quadrature to the source signal $s(t)$.

$$e_s(t) = j\sqrt{\left[\frac{c_{\max}^2}{|s(t)|^2} - 1\right]}. \tag{3}$$

Thus

$$s(t) = s_1(t) + s_2(t) \quad \text{and} \quad |s_1(t)| = |s_2(t)|. \tag{4}$$

The amplifier of each path is characterized by a level-dependent complex gain, with an output signal in each path given by

$$s_{o1}(t) = v_1(t) \cdot G_1(|v_1(t)|) \quad s_{o2}(t) = v_2(t) \cdot G_2(|v_2(t)|). \tag{5}$$

Where $v_1(t)$ and $v_2(t)$ are the baseband representation of the instantaneous complex envelope amplifier input signal in each path.

Therefore, if the D-to-A converters and quadrature modulators are supposed to be ideal, that is, $s_1(t) = v_1(t)$ and $s_2(t) = v_2(t)$, and both signals $s_{o1}(t)$ and $s_{o2}(t)$ are properly added in phase, the output signal in complex format then becomes

$$\begin{aligned} s_o(t) &= s_{o1}(t) + s_{o2}(t) \\ &= s_1(t) \cdot G_1(|v_1(t)|) + s_2(t) \cdot G_2(|v_2(t)|) \\ &= s(t) \cdot \frac{G_1(|v_1(t)|) + G_2(|v_2(t)|)}{2} \\ &\quad + e_s(t) \cdot \frac{G_1(|v_1(t)|) - G_2(|v_2(t)|)}{2}. \end{aligned} \tag{6}$$

The second term in (6) implies that there is an unwanted residual signal due to imperfect cancellation (it tends to zero as the gain and phase matching are perfected). The term introduces interfering power in the adjacent channel limiting the spectrum efficiency of the system.

The aim of this method is to reduce the factor $[G_1(|v_1(t)|) - G_2(|v_2(t)|)]$ as much as possible. The method is based on adaptive signal processing techniques and its main advantage is to track input signal variations and possible changes due to temperature variations, amplifier bias and component aging, among others.

III. Correction Method Model

A schematic diagram of the simulation model is depicted in Fig. 2. The source signal is separated into the two constant-envelope signals, given in (2), by an SCS. These signals are multiplied by different complex coefficients, one for each branch (K_1 and K_2). These coefficients are computed and continuously updated to reduce the Adjacent Channel Interference by means of an adaptive algorithm. This algorithm needs a reference of the output signal to update the complex coefficients. A feedback signal, $r(t)$ is obtained by means of a downconversion process of the output power amplifier signal $s_o(t)$, where $1/G_L$ is the downconversion gain, including the output coupler gain. This downconversion gain allows adjusting the range of signal values to the quadrature demodulator input and it is defined as the mean of the amplifying branches gain.

The adaptation criterion of the algorithm is to minimize the mean-squared-error. The error signal defined by (7) is the difference between the source signal, $s(t)$, and the feedback signal, $r(t)$.

$$e(t) = s(t) - r(t). \tag{7}$$

The feedback signal can be written as

$$\begin{aligned} r(t) &= \frac{s_o(t)}{G_L} \\ &= \frac{s_1(t) \cdot K_1 \cdot G_1(|v_1(t)|) + s_2(t) \cdot K_2 \cdot G_2(|v_2(t)|)}{G_L}. \end{aligned} \tag{8}$$

Substituting (4) and (8) into (7), the error signal can be written as the addition of two error signals, $e_1(t)$ and $e_2(t)$.

$$e(t) = e_1(t) + e_2(t) \tag{9}$$

$$e_1(t) = s_1(t) - \frac{s_1(t) \cdot K_1 \cdot G_1(|v_1(t)|)}{G_L} \tag{10}$$

$$e_2(t) = s_2(t) - \frac{s_2(t) \cdot K_2 \cdot G_2(|v_2(t)|)}{G_L}. \tag{11}$$

Where ideal D-to-A, A-to-D converters, quadrature modulators/demodulator and a null loop delay, τ, are assumed.

The cost function to minimize is defined as

$$J = E\left[|e(t)|^2\right]. \tag{12}$$

Where E[.] denotes the statistical expectation operator.

For simpler notation, in following formulae, $G_1(|v_1(t)|)$ and $G_2(|v_2(t)|)$ will be denoted as G_1 and G_2.

The gradient of the cost function is calculated as

$$\nabla_{K_n} J = \frac{\partial J}{\partial Kr_n} + j\frac{\partial J}{\partial Ki_n} \text{ With } K_n = Kr_n + jKi_n \;\; n = 1, 2. \tag{13}$$

Where Kr_n denotes the real part and Ki_n the imaginary part of K_n.

For the cost function J to attain its minimum value, all the terms of the gradient must be simultaneously equal to zero.

Computing the cost function (12) gives

$$\begin{aligned} J = E[e(t) \cdot e^*(t)] &= E[e_1(t) \cdot e_1^*(t)] + E[e_2(t) \cdot e_1^*(t)] \\ &\quad + E[e_1(t) \cdot e_2^*(t)] + E[e_2(t) \cdot e_2^*(t)]. \end{aligned} \tag{14}$$

The partial derivatives with respect to Kr_n and Ki_n are calculated to obtain the gradient of the cost function defined by (13). Approximating the terms with derivation variable K_n toward zero in the work region of the amplifier, finally we obtain

$$\nabla_{k_n} J \approx -2 \cdot E\left[e(t) \cdot s_n^*(t) \cdot \frac{G_n^*}{G_L^*}\right] \quad n = 1, 2. \tag{15}$$

The cost function depends on two signals, the error signal, $e(t)$ available in the digital processing block and the signal defined

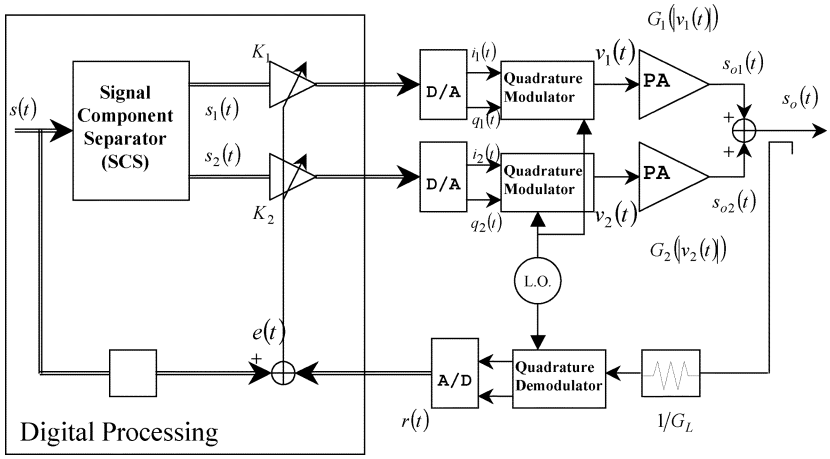

Fig. 2. Simulation model.

by $[s_n^*(t)\cdot(G_n^*/G_L^*)]$. This last signal is not available in the proposed model, but according to the downconversion gain definition, we can use the approximation $G_n \approx G_L$, and thus the expression (15) can be written as

$$\nabla_{k_n} J \approx -2\cdot E\left[\, e(t)\cdot s_n^*(t)\right] \quad n=1,2. \tag{16}$$

Therefore, using the instantaneous estimate of the gradient, the updated value of the adaptive coefficient at time $\mathrm{m}+1$ is computed by using the simple recursive relation

$$K_n(m+1) = K_n(m) + \mu_n \cdot e(m)\cdot s_n^*(m) \quad n=1,2. \tag{17}$$

Where the positive real-valued constant μ_n (step-size), controls the speed of convergence and the misadjustment (final excess error) of the algorithm.

IV. Simulations

A. OFDM Modulation

The source signal for simulations was an OFDM signal, similar to the OFDM signal defined in the DVB-T standard [16], with the following parameters:

- 2 K mode:1705 active subcarriers
- Subcarrier Spacing: 4.464 KHz
- Useful Symbol Duration: 224 μs
- Constellation: 16 QAM

The modulated OFDM signal during a symbol can be expressed as follows

$$s(t) = e^{j2\pi f_c t}\sum_{k=K_{\min}}^{K_{\max}} c_{0,0,k}\quad e^{j2\pi k'(t-\Delta)/T_u}$$
$$\text{with } k' = k - \frac{(K_{\max}+K_{\min})}{2}. \tag{18}$$

T_u is the inverse of the carrier spacing, Δ is the duration of the guard interval, k denotes the carrier number, f_c is the central frequency of the RF signal and $c_{0,0,k}$ is a complex symbol for carrier k.

There is a clear resemblance between this and the inverse Discrete Fourier Transform (DFT)

$$x[n] = \frac{1}{N}\sum_{k=0}^{N-1} X[k]\, e^{j2\pi k(n/N)}. \tag{19}$$

Since various efficient Fast Fourier Transform algorithms exist to perform the DFT and its inverse, it is a convenient form of implementation to use the inverse FFT (IFFT) in a DVB-T modulator to generate N samples $x[n]$ corresponding to the useful part, T_u long, of each symbol. The guard interval is added by taking copies of the last $N\Delta/T_u$ of these samples and appending them in front. This process is then repeated for each symbol in turn, producing a continuous stream of samples, which constitutes a complex baseband representation of the DVB-T signal. A subsequent up-conversion process then gives the real signal $s(t)$ centred on the frequency, f_c.

B. Amplifier Model

The amplifier is characterized by a complex gain using a memoryless model, which depends on the input signal level. A common method to model power amplifiers taking into account nonlinearities with memory is to use a Volterra series representation. For most amplifiers, where the modulation bandwidth is much less than the carrier frequency, the memory in the nonlinearity is small enough to be neglected, and the Volterra series can be simplified into a simple power series with complex coefficients [18]. The complex gain of the amplifier is extracted from AM-AM and AM-PM characteristics of a class AB amplifier. The Class AB power amplifier design is simulated using the model of the LX802 LDMOS transistor from Polyfet [27] (with a driver) at 600 MHz (50 Ω system). A polynomic regression is used to model the amplifier complex gain of each path.

$$G_n(|v(t)|) = M_n(|v(t)|)\cdot e^{j\Phi_n(|v(t)|)} \quad n=1,2 \tag{20}$$

$$\begin{aligned} M_n(|v(t)|) = {} & 192.30\cdot\alpha_{n,1} + 91.83\cdot\alpha_{n,2}\cdot|v(t)| \\ & -736.80\cdot\alpha_{n,3}\cdot|v(t)|^2 + 907.01\cdot\alpha_{n,4}\cdot|v(t)|^3 \\ & -490.95\cdot\alpha_{n,5}\cdot|v(t)|^4 + 124.72\cdot\alpha_{n,6}\cdot|v(t)|^5 \\ & -12.11\cdot\alpha_{n,7}\cdot|v(t)|^6 \end{aligned} \tag{21}$$

$$\begin{aligned} \Phi_n(|v(t)|) = {} & -1.9758\cdot\beta_{n,1} + 0.9181\cdot\beta_{n,2}\cdot|v(t)| \\ & -2.0892\cdot\beta_{n,3}\cdot|v(t)|^2 + 1.7987\cdot\beta_{n,4}\cdot|v(t)|^3 \\ & -0.7584\cdot\beta_{n,5}\cdot|v(t)|^4 + 0.1557\cdot\beta_{n,6}\cdot|v(t)|^5 \\ & -0.0124\cdot\beta_{n,7}\cdot|v(t)|^6. \end{aligned} \tag{22}$$

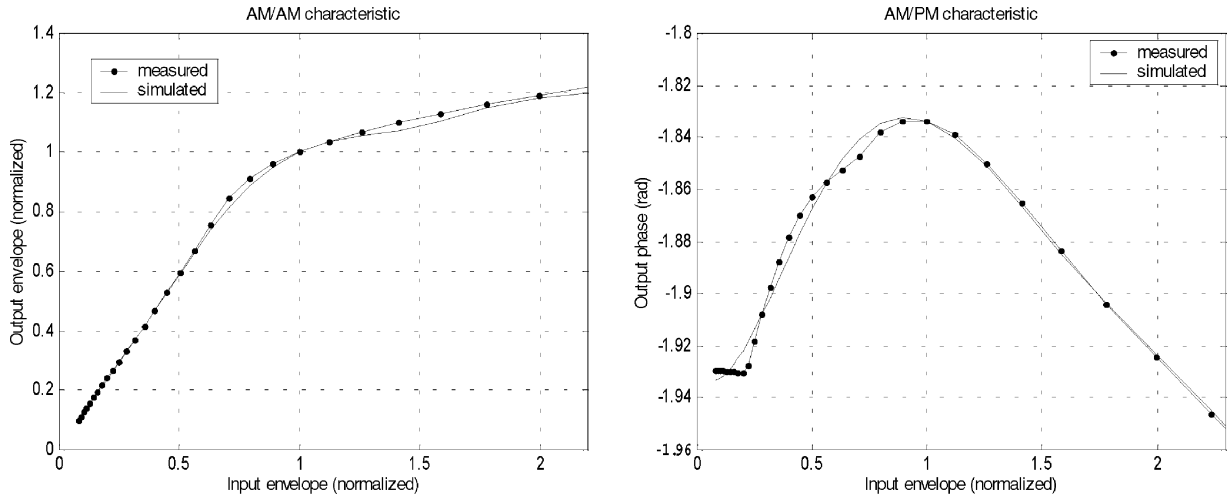

(a) (b)

Fig. 3. (a) AM/AM and (b) AM/PM characteristics of the designed class AB amplifier and the corresponding polynomic regression model.

The amplifier in path 1 is characterized with the parameters $\alpha_{1,\mathrm{j}}, \beta_{1,\mathrm{j}}$ equal to 1. The amplifier in path 2 is modeled modifying appropriately factors $\alpha_{2,\mathrm{j}}$ and $\beta_{2,\mathrm{j}}$ to simulate the inclusion of gain and phase imbalances between both amplifying branches.

Fig. 3 shows the AM/AM and AM/PM characteristics (normalized to the 1 dB compression point) of the designed class AB power amplifier and the corresponding calculated polynomic regression model, which is used to simulate the amplifier of path 1.

The downconversion gain was simulated as an estimation of the inverse of the total equivalent linear gain of the amplifier stage (mean of the equivalent linear gain of the amplifier in path 1 and the one in path 2).

C. Transmit Signal Power Spectrum Performance

Due to the coexistence of many digital and analog broadcast signals in the whole service bandwidth, the requirements respect to the spectrum level outside the channel bandwidth are determinated in the standard DVB-T through spectrum emission templates. For example, the spectrum level at frequency offset of 4.2 MHz from the center frequency is at least 36 dB lower than the center spectrum level. Fig. 4 shows the normalized power spectral density (PSD) of the output power amplifier signal, $S_o(f)$ for different values of Output Power Back-off (OBO) with a single amplifying branch, that is, without a transmitter LINC structure and for a 16-QAM modulated OFDM input signal operating at a sampling frequency of 29.25 MHz.

According to Fig. 4, the requirement of an attenuation of 36 dB in 4.2 MHz is obtained for OBOs larger than 10 dB, which implies low power efficiency. The proposed power amplifier (with a driver) is designed to optimize the 1 dB compression output power ($\mathrm{P}_{\mathrm{out\_1\,dB}} = 45.4\,\mathrm{dBm}$), resulting its Power Added Efficiency (PAE), $\eta_a = 60\%$, where

$$\eta_a = \frac{P_{RF\_OUT} - P_{RF\_IN}}{P_{DC}}. \tag{23}$$

With a single amplifying branch the total efficiency is [28], [29]

$$\eta_{tot} = \eta_a \cdot \eta_m \tag{24}$$

where η_m is the modulation scheme efficiency.

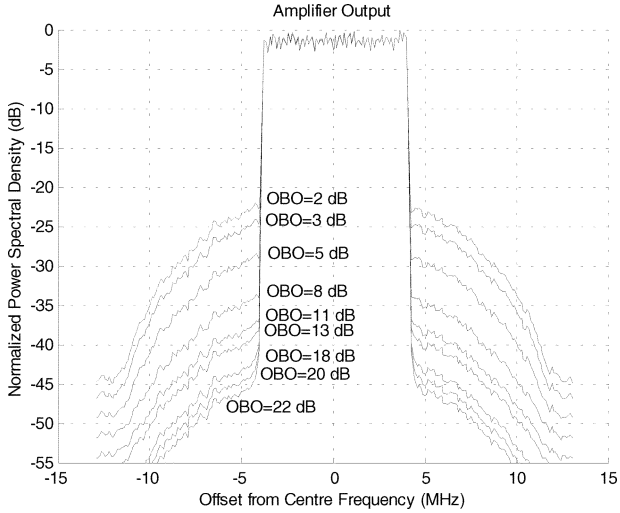

Fig. 4. Normalized power spectral density of simulated amplifier output signal for different values of OBO (with a single amplifying branch).

The proposed amplifier has a PAE value equal to 17% at 10 dB OBO related to the 1 dB compression point, which supposes a great efficiency reduction to achieve the required Adjacent Channel Protection (ACP).

To realize the full power efficiency potential of LINC technique, not only the PAs but also the recombination process must be highly efficient. Typically, a hybrid combiner, with the loss on power efficiency due to the wasted at heat in the load match, is used. The possibility of reducing this drawback effect by recycling otherwise wasted energy using a RF-DC converter to partially recover the wasted energy has been studied [30]. Other combiners proposals are based on the Wilkinson combiner without isolation resistor [31]. Some studies about the appropriate susceptance presented to the power amplifier in this scheme, are described in [32], [33]. This susceptance value can be automatically adjusted as proposed in [34]. Taking into account the combiner efficiency, the total system efficiency can be written as

$$\eta_{tot} = \eta_a \cdot \eta_m \cdot \eta_c. \tag{25}$$

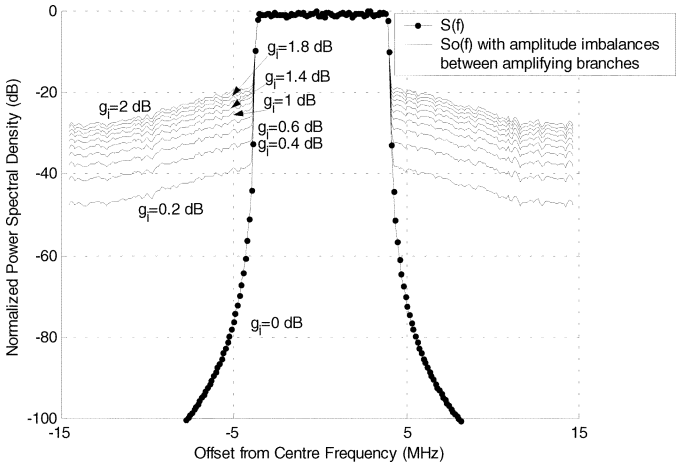

Fig. 5. Normalized power spectral density of simulated input $S(f)$ and output $S_o(f)$ with several gain imbalances ($0 \leq g_i \leq 2$ dB) and without phase imbalance in the second branch of a LINC transmitter (without a correction method).

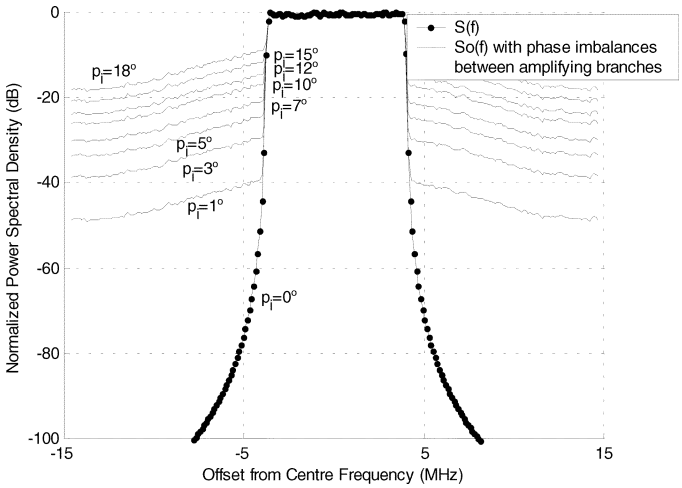

Fig. 6. Normalized power spectral density of simulated input $S(f)$ and output $S_o(f)$ with several phase imbalances ($0° \leq p_i \leq 18°$) and without gain imbalance in the second branch of a LINC transmitter (without a correction method).

η_m and η_c are not the objective of this paper, since they have been widely treated in above referenced works.

As mentioned before, in order to increase the power efficiency, an adaptive LINC transmitter scheme is proposed. If an ideal transmitter LINC structure is applied, that is, the two amplifying branches are equal, the nonlinear distortion cancellation is almost perfect, but in a realistic situation, where there are gain and phase imbalances between both amplifying branches, the power spectral density of the output power amplifier signal $S_o(f)$ is degraded as Figs. 5 and 6 show.

In all the following presented results a 5 dB OBO at the output combiner is applied.

Figs. 5 and 6 illustrate the effect of gain and phase imbalances and the need for a method to achieve gain and phase matching as presented in this paper. It can be seen that a slight gain or phase imbalance between both amplifying branches worsens the LINC transmitter performance.

Fig. 7 compares the normalized input and output power spectral density with and without the presented adaptive correction

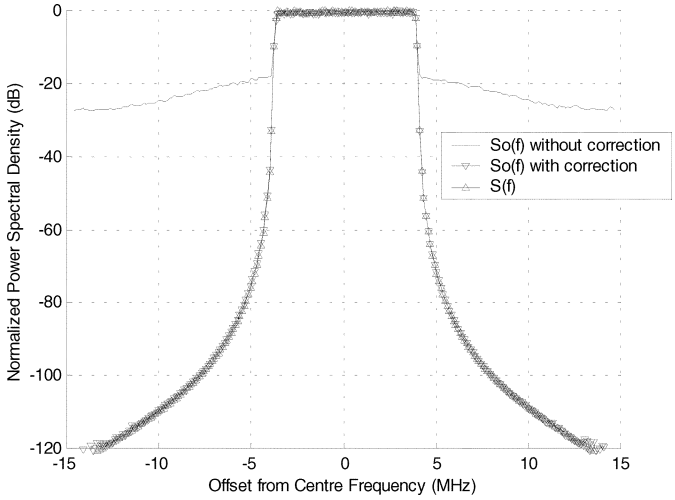

Fig. 7. Normalized power spectral density of simulated input $S(f)$ and output $S_o(f)$ with and without correction(with 1.5 dB gain and 5° phase imbalances between both amplifying branches).

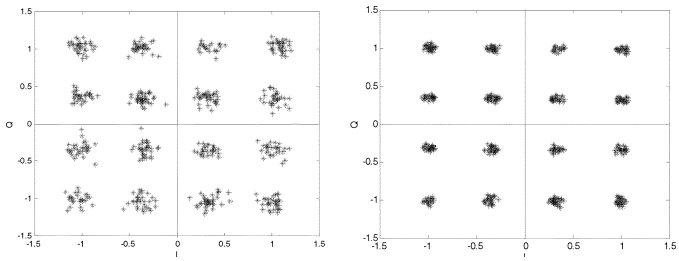

Fig. 8. Received signal constellation diagram (normalized) (a) without imbalances correction method (b) with the proposed correction method.

method and using a 1.5 dB gain imbalance and a 5° phase imbalance between both amplifying branches.

As it can be seen in Fig. 7, the Adjacent Channel Interference is reduced after applying the correction method with accurate gain and phase matching between the two paths.

The Error Vector Magnitude (EVM) is another important transmission requirement in digital communication systems. The effects of the gain and phase imbalances on the vector error may be analyzed as follows

$$EVM = \sqrt{(R^2 + M^2) - 2RM\cos(\alpha_e)} \tag{26}$$

where R is the magnitude of the 'ideal' vector, M is the magnitude of the measured vector, and α_e is the phase error between them. The measured vector magnitude, M, is composed of the 'ideal' magnitude, R, plus a component resulting from the gain error present in the system, G_e. Therefore, (26) can be written as

$$EVM = \sqrt{\left(R + (R + G_e)^2\right) - 2R(R + G_e)\cos(\alpha_e)}. \tag{27}$$

The 16-QAM received signal constellation without and with the correction method for a LINC transmitter are depicted in Fig. 8(a) and (b), respectively. The EVM improves after the proposed correction method is applied. ($\mathrm{EVM} \approx 8\%$ without the correction method, $\mathrm{EVM} \approx 3.5\%$ with the correction method)

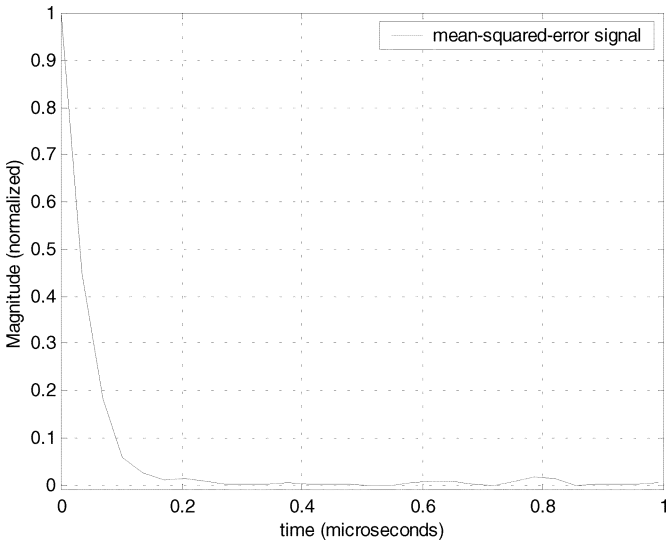

Fig. 9. Evolution of the mean-squared-error signal.

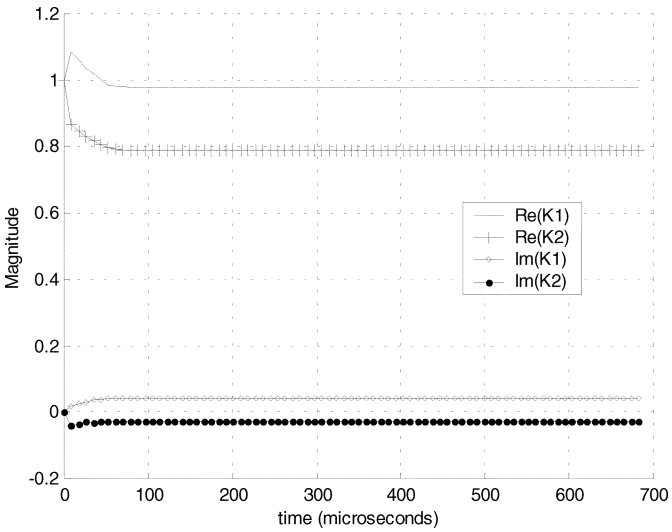

Fig. 10. Value range of adaptive coefficients, K_1 and K_2.

Using this method, the speed of convergence can be measured by analyzing the time evolution of the mean-squared-error. Taking into account that the speed convergence depends on the step size parameter, μ_n, this parameter has been chosen in order to reduce the ACI value as far as possible. As Fig. 9 shows, the convergence time can be considered lower than 0.5 μs, that is, much lesser than the symbol time, 280 μs. Therefore, this method can be suitable for real time implementation.

We have also analyzed whether the value range of adaptive coefficients is suitable for its implementation in a digital processor. Fig. 10 shows the value range of the real and imaginary part of the coefficients, K_1 and K_2. It demonstrates that the value range of both adaptive coefficients along time is delimited and it is appropriate in order to be implemented in any digital processor device.

V. Nonideal System Model

Now a set of nonidealities must be introduced in order to deal with a more realistic model: an error in the estimation of the downconversion gain and the impairments of quadrature modulators and demodulator.

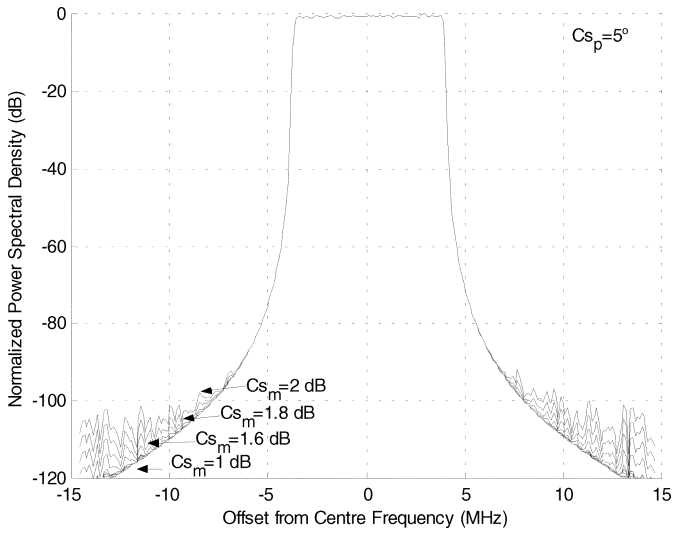

Fig. 11. Normalized power spectral density of simulated output $S_o(f)$ with different amplitude errors in the estimation of the downconversion gain.

A. Error in the Downconversion Gain Estimation

As mentioned above, the downconversion gain, G_L, is simulated as an estimation of the inverse of total equivalent linear gain of the amplifying branches. It is calculated as the mean of the gain amplifying branches, G_t. Now, we consider how an error in the downconversion gain estimation influences on the performance of this method. Fig. 10 shows the results of the simulations carried out introducing amplitude and phase errors, Cs, in the calculated downconversion gain, G_t, using the expression (28).

$$G_L = G_t \cdot Cs \qquad Cs = Cs_m \cdot e^{jCs_p}. \tag{28}$$

It can be seen that amplitude errors in the downconversion gain estimation below 1 dB do not influence the system performance. The influence increases slowly when the amplitude errors are above 1.5 dB, but even for higher values, the generated ACI is negligible.

B. Modulator and Demodulator Misalignments

Perfectly balanced quadrature modulators and demodulator were assumed in this architecture, which leads to another practical consideration. The quadrature imbalances (amplitude and phase) create a residue in the adjacent channel, increasing the ACI [19], [26]. Fig. 12(a) shows the degradation of the ACI when there are amplitude imbalances in the quadrature modulators, without phase imbalance and Fig. 12(b) shows the phase imbalances effect without amplitude imbalance. There is a strong influence of the imbalances of the quadrature modulator on the system performance, and it can become a limitation in this architecture.

We have also analyzed the effect of an unbalanced quadrature demodulator in this architecture. Fig. 13(a) and 13(b) show the influence of the imbalances in the quadrature demodulator on the proposed method and architecture.

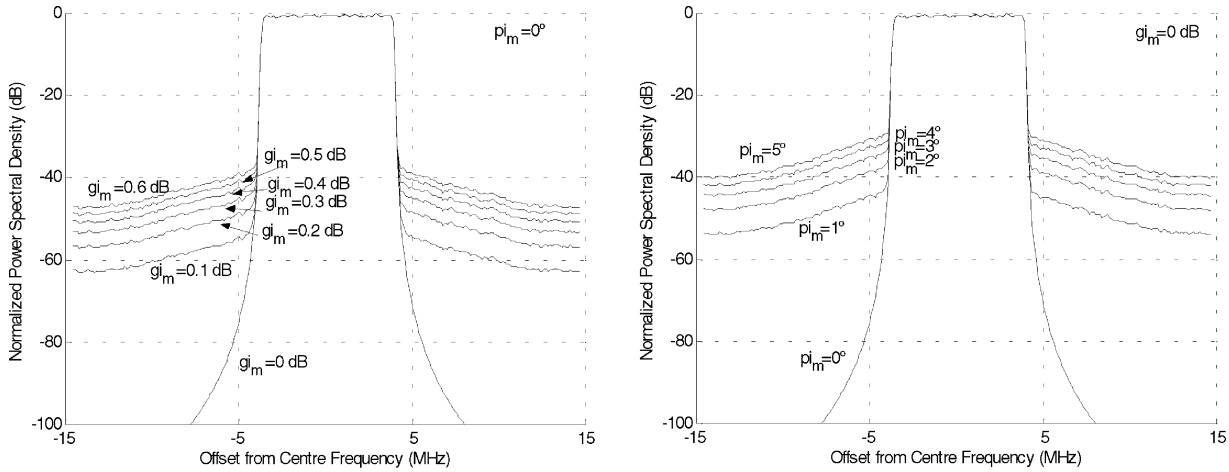

Fig. 12. Normalized power spectral density of simulated output $S_o(f)$ (a) with amplitude imbalances (b) with phase imbalances in the quadrature modulator.

Fig. 14 shows the effect in the distortion in the adjacent channel of a more realistic model with the following commercial values of imbalances in the quadrature modulators/demodulator.

The reduction in the adjacent channel interference using the proposed adaptive LINC transmitter with regard to a single amplifying branch is almost 18 dB. There are two possible solutions if a greater increase is required. One of them involves the use of perfect digital modulators/demodulator or their integration in an ASIC device in order to get lower misalignments in the modulators and demodulator. The other one means performing some techniques for correction of the analogue modulators and the demodulator. This paper does not focus in the quadrature modulator and demodulator correction networks. Several publications have addressed this matter [21]–[24].

Anyway, the requirements of DVB-T standard regarding the spectrum level outside the channel bandwidth are broadly fulfilled. It would be also possible to reduce the Output Power Backoff using the proposed method and therefore higher power efficiency would be obtained. Fig. 15 shows the PSD of the output power amplifier signal, $S_o(f)$, for different values of Output Power Back-off (OBO) applying the proposed adaptive transmitter LINC method. According to Fig. 15, thanks to this method it would be possible to work with a 2 dB OBO fulfilling the requirements of DVB-T standard.

The comparison between Figs. 15 and 4, with a 5 dB OBO, demonstrates that this method improves the out-of-band spurious rejection around 18 dB. In this situation, the amplifier efficiency is $\eta_a = 34\%$. The same performance can be obtained with a single amplifier structure, operating at a 20 dB OBO, which would imply very low power efficiency, that is, $\eta_a = 3\%$. Besides, the amplifier efficiency in the proposed adaptive transmitter LINC method, for a 2 dB OBO, is $\eta_a = 49\%$, and a 15 dB OBO is required to obtain the same performance with a single amplifying branch, which supposes an amplifier efficiency $\eta_a = 7\%$.

On the other hand, in the overall efficiency of this scheme the power consumption of the adaptive signal processing has to be included. The proposed technique consists of two signal-processing blocks: the Signal Component Separator, typical of a LINC transmitter, and the adaptive correction method. The implementation of the SCS block has been treated in previous publications [35], where the design of this block by means of an application-specific signal processor (ASDSP) to reduce the power consumption is suggested. The adaptive correction method is an algorithm with simple multiplications and additions instructions. Therefore, it can be implemented using any current DSP with a very low number of instructions (less than 20), which implies a low power consumption (for a typical DSP consumption 1,4 mW/MIPS), with regard to the consumption in the power stages. It supposes a reduction in the overall efficiency from 49% to 48%. Anyway, this block can be also implemented using an ASDSP in order to further decrease the power consumption.

Therefore, an overall efficiency increase greater than 40% is obtained when the proposed adaptive correction method is applied.

Another ideal situation that has been assumed in the previous simulations corresponds to a null loop delay. The feedback signal $r(t)$ is a delayed and attenuated version of the amplifier output signal $s_o(t)$. Including in (8) the loop delay, τ, the feedback signal can be written as

$$r(t) = \frac{s_o(t-\tau)}{G_L}. \tag{29}$$

The delay must be compensated for the adaptive algorithm to correctly compare the source signal, $s(t)$, with the feedback signal, $r(t)$. As the digital processing block contains both signals, a delay compensation can be easily made by means of an appropriate comparison between both signals, as shows (30)

$$e(t) = s(t-\tau) - r(t). \tag{30}$$

Therefore, the delay produced by the correction circuit has to be estimated before introducing the adaptive algorithm. A rough estimation can be carried out with the theoretical time delay of the components in the design or by applying some of the loop delay estimation techniques proposed by other authors [18], [21], [25] or with some previous calibration.

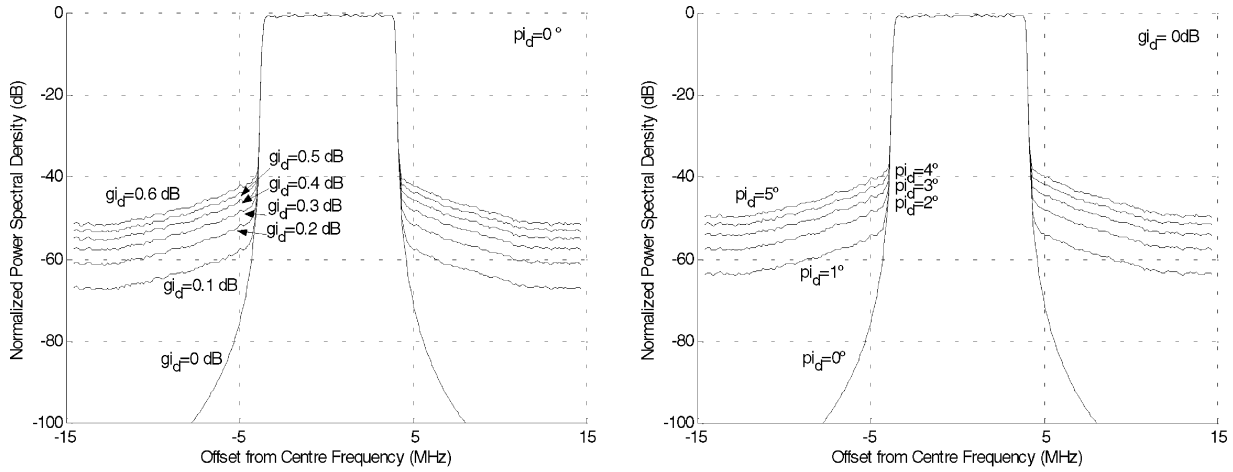

(a) (b)

Fig. 13. Normalized power spectral density of simulated output $S_o(f)$ (a) with amplitude imbalances (b) with phase imbalances in the quadrature demodulator.

	Amplitude imbalance	*Phase imbalance*
I/Q Modulator path 1	0.15 dB	1°
I/Q Modulator path 2	0.1 dB	1.5 °
I/Q Demodulator	0.3 dB	1.3°

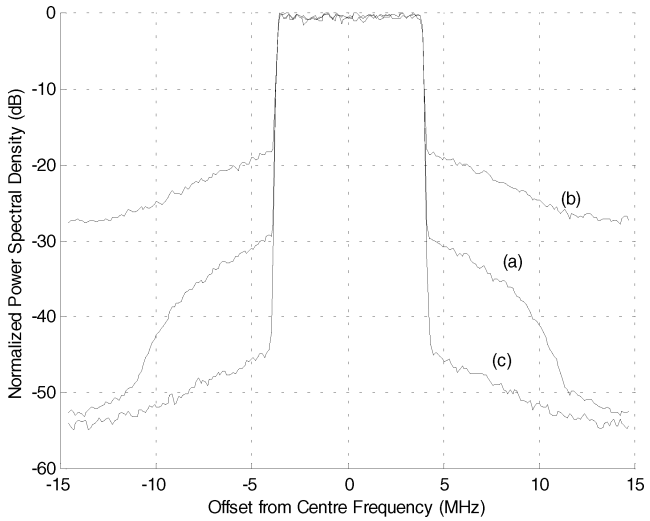

Fig. 14. Normalized power spectral density of simulated output signal $S_o(f)$ with imbalances in quadrature modulators and demodulator in three situations: (a) with a single amplifying branch (without LINC transmitter) (b) with LINC transmitter but without imbalances correction method between amplifying branches and (c) with LINC transmitter and applying the proposed correction method.

We have analyzed the influence of errors in the estimation of the loop delay. According to the results showed in Fig. 16, the adaptive method runs correctly if the error in the delay estimation is less than 1 μs. So, accurate delay matching is important to improve the performance of this method, but it is not a limitation when implementing it in a real system.

VI. Conclusion

We have investigated the applicability for OFDM transmission systems of an adaptive digital method of amplifier

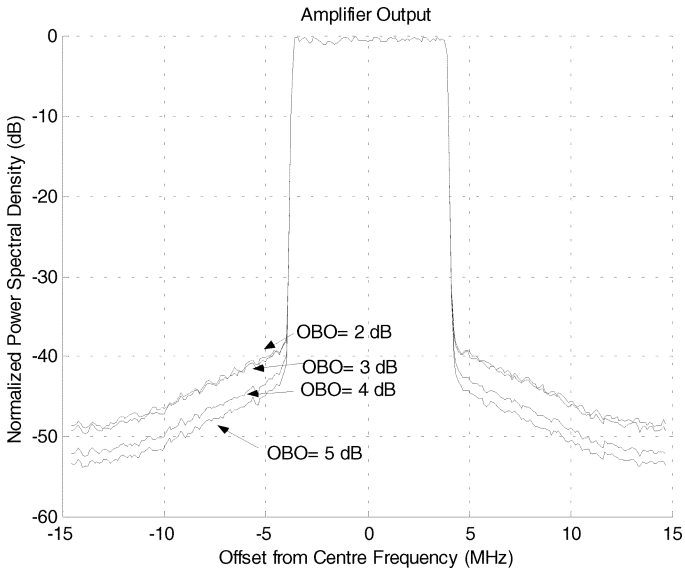

Fig. 15. Normalized power spectral density of simulated output amplifier for different values of OBO with the proposed adaptive transmitter LINC method.

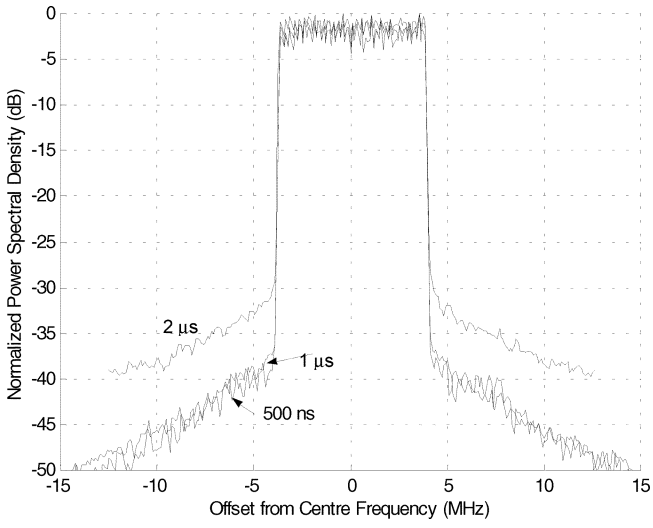

Fig. 16. Normalized PSD of the simulated output signal, $S_o(f)$, with errors in the estimation of the loop delay.

linearization, based on a LINC transmitter scheme, in order to reduce the nonlinear distortion. The presented method corrects the undesirable gain and phase imbalances, which appear between amplifying branches in LINC transmitters. Using a simulation we have demonstrated that it is possible to reduce the Adjacent Channel Interference around 18 dB in a system with a multicarrier modulation, working at a 2 dB OBO. The same performance can be obtained with a single amplifier structure, operating at a 15 dB OBO, which implies an efficiency increase greater than 40%. The proposed model converges quickly toward very low interference levels in adjacent channels. According to the simulation, the adaptive coefficients quickly reach its optimal value. Effects of system impairments, such as modulator and demodulator misalignments and loop delay have been also included. As a result of its adaptive technique, this method can track the input signal variations and possible changes due to variations in operating conditions.

REFERENCES

[1] R. van Nee and R. Prasad, *OFDM for Wireless Multimedia Communications*: Ed. Artech House, 2000.

[2] P. Banelli, G. Baruffa, and S. Cacopardi, "Effects of HPA non linearity on frequency multiplexed OFDM signals," *IEEE Trans. Broadcast.*, vol. 47, no. 2, pp. 123–136, Jun. 2001.

[3] A. Chini, Y. Wu, M. El-Tanany, and S. Mahmoud, "Hardware nonlinearities in digital TV broadcasting using OFDM modulation," *IEEE Trans. Broadcast.*, vol. 44, no. 1, pp. 12–21, Mar. 1998.

[4] E. Costa, M. Midrio, and S. Pupolin, "Impact of amplifier nonlinearities on OFDM transmission system performance," *IEEE Commun. Lett.*, vol. 3, pp. 37–39, Feb. 1999.

[5] P. Banelli and G. Baruffa, "Mixed BB-IF predistortion of OFDM signals in nonlinear channels," *IEEE Trans. Broadcast.*, vol. 47, no. 2, pp. 137–146, Jun. 2001.

[6] A. N. Andrea, V. Lottici, and R. Reggiannini, "Nonlinear predistortion of OFDM signals over frequency-selective fading channels," *IEEE Trans. Commun.*, vol. 49, no. 5, pp. 837–843, May 2001.

[7] H. W. Kang, Y. S. Cho, and D. H. Youn, "On compensating nonlinear distortions of an OFDM system using an efficient adaptive predistorter," *IEEE Trans. Commun.*, vol. 47, no. 4, pp. 522–526, Apr. 1999.

[8] W. G. Jeon, K. H. Chang, and Y. S. Cho, "An adaptive data predistorter for compensation of nonlinear distortion in OFDM systems," *IEEE Trans. Commun.*, vol. 45, pp. 1167–1171, Oct. 1997.

[9] F. J. Casadevall and A. Valdovinos, "Performance analysis of QAM modulations applied to the LINC transmitter," *IEEE Trans. Veh. Technol.*, vol. 42, no. 4, pp. 399–406, Nov. 1993.

[10] F. J. Casadevall and J. J. Olmos, "On the behavior of the LINC transmitter," in *Proc. 40th IEEE Veh. Technol. Conf.*, Orlando, May 1990, pp. 29–34.

[11] S. Tomisato, K. Chiba, and K. Murota, "Phase error free LINC modulator," *Electron. Lett.*, vol. 25, no. 9, pp. 576–577, Apr 1989.

[12] L. Sudström, "Automatic adjustment of gain and phase imbalances in LINC transmitters," *Electron. Lett.*, vol. 31, no. 3, pp. 155–156, Feb. 1995.

[13] S. Ampem-Darko and H. S. Al-Raweshidy, "Gain/phase imbalance cancellation technique in LINC transmitters," *Electron. Lett.*, vol. 34, no. 22, pp. 2093–2094, Oct. 1998.

[14] X. Zhang, L. E. Larson, P. M. Asbeck, and P. Nanawa, "Gain/phase imbalance-minimization techniques for LINC transmitter," *IEEE Trans. Microw. Theory and Techniques*, vol. 49, no. 12, pp. 2507–2516, Dec. 2001.

[15] S. A. Hetzel, A. Bateman, and J. P. McGeehan, "LINC transmitter," *IEEE Electron. Lett.*, vol. 27, no. 10, pp. 844–846, May 1991.

[16] "Framing Structure, Channel Coding and Modulation for Digital Terrestrial Television," ESTI EN 300 744—Digital Video Broadcasting (DVB), v1.4.1 (2001–01).

[17] R. Dinis and A. Gusmao, "Signal processing schemes for power/bandwidth efficient OFDM transmission with conventional or LINC transmitter structures," in *IEEE Int. Conf. Communications, ICC*, vol. 4, Jun. 2001, pp. 1021–1027.

[18] J. de Mingo and A. Valdovinos, "Performance of a new digital baseband predistorter using calibration memory," *IEEE Trans. on Veh. Tech.*, vol. 50, no. 4, pp. 1169–1176, Jul. 2001.

[19] J. K. Cavers, "The effect of quadrature modulator and demodulator errors on adaptive digital predistorters for amplifier linearization," *IEEE Trans. Veh. Technol.*, vol. 46, pp. 456–466, May 1997.

[20] P. B. Kenington, *High-Linearity RF Amplifier Design*: Ed. Artech House, 2000.

[21] J. K. Cavers, "New methods for adaptation of quadrature modulators and demodulator in amplifier linearization circuits," *IEEE Trans. Veh. Technol.*, vol. 46, no. 3, pp. 707–716, Aug. 1997.

[22] M. Faulkner, T. Mattson, and W. Yates, "Automatic adjustment of quadrature modulators," *Electron. Lett.*, vol. 27, no. 3, pp. 214–216, Jan. 1991.

[23] M. Faulkner and M. Johansson, "Correction of mixer nonlinearity in quadrature modulators," *Electron. Letter*, vol. 28, no. 3, pp. 293–295, Jan. 1992.

[24] J. K. Cavers and M. W. Liao, "Adaptive compensation for imbalance and offset losses in direct conversion transceivers," *IEEE Trans. Veh. Technol.*, vol. 42, pp. 581–588, Nov. 1993.

[25] A. S. Wrigth and W. G. Durtler, "Experimental performance of and adaptive digital linearized power amplifier," *IEEE Trans. Veh. Technol.*, vol. 43, pp. 323–332, May 1994.

[26] L. Sundström, "Spectral sensitivity of LINC transmitters to quadrature modulator misalignments," *IEEE Trans. Veh. Technol.*, vol. 49, no. 4, pp. 1474–1487, Jul. 2000.

[27] . [Online]. Available: http://www.polyfet.com

[28] L. Sundström and M. Johansson, "Effect of modulation scheme on LINC transmitter power efficiency," *Electron. Lett.*, vol. 30, no. 20, pp. 1643–1645, Sep. 1994.

[29] B. Shi and L. Sundström, "Investigation of highly efficient LINC amplifier topology," in *Veh. Technol. Conf. 2001, VTC 2001 Fall IEEE VTS 54th*, vol. 2, Oct. 2001, pp. 1215–1219.

[30] R. Langridge, T. Thornton, P. M. Asbeck, and L. E. Larson, "A power re-use technique for improved efficiency of outphasing microwave power amplifiers," *IEEE Trans. Microw. Theory and Techniques*, vol. 47, no. 8, pp. 1467–1470, Aug. 1999.

[31] C. P. Conradi, R. H. Johnston, and J. G. McRory, "Evaluation of a lossless combiner in LINC transmitter," in *IEEE Canadian Conf. Electrical and Computer Engineering*, vol. 1, May 1999, pp. 105–110.

[32] B. Stengel and W. R. Eisenstadt, "LINC power amplifier combiner method efficiency optimization," *IEEE Trans. Veh. Technol.*, vol. 49, no. 1, Jan. 2000.

[33] F. H. Raab, "Efficiency of outphasing RF power-amplifier systems," *IEEE Trans. Commun.*, vol. Com-33, pp. 1094–1099, Oct. 1985.

[34] J. de Mingo, A. Valdovinos, A. Crespo, D. Navarro, and P. Garcia, "An RF electronically controlled impedance tuning network design and its application to an antenna input impedance automatic matching system," *IEEE Trans. Microw. Theory and Techniques*, vol. 52, no. 2, Feb. 2004.

[35] L. Sundström, "The effect of quantization in a digital signal component separator for LINC transmitters," *IEEE Trans.Veh. Technol.*, vol. 45, no. 2, pp. 346–352, May 1996.

Paloma García was born in Zaragoza, Spain, in 1972. She received the Engineer of Telecommunications degree from the University of Zaragoza (Spain) in 1996. In 1995 she was employed in TELTRONIC SAU where she worked in the Research and Development Department, involved in the design of radio communication systems (mobile equipment and base station) until 2002.

Since 1997 until 2001, she has collaborated in several projects with the Communication Technologies Group of the Electronics Engineering and Communications Department in the University of Zaragoza. In 2002, she joined the Centro Politécnico Superior, University of Zaragoza, where she is an Assistant Professor. His research interests are in the area of linearization techniques of power amplifiers, and signal processing techniques for radio communication systems.

Alfonso Ortega was born in Teruel, Spain, in 1976. He received the M. Sc. degree in Telecommunication Engineering from the University of Zaragoza (UZ), Spain, in 2000.

In 1999 he joined, under a research grant, the Communications Technologies Group (UZ) where he has been an Assistant Professor since 2001. He is also involved as a researcher with the Aragon Institute of Engineering Research (I3A). At present his research interest lies in the field of adaptive signal processing applied to radio communication systems and speech technologies.

Jesús de Mingo (M'98) was born in Barcelona, Spain, in 1965. He received the "Ingeniero de Telecomunicación" degree from the "Universidad Politécnica de Cataluña" (UPC), Barcelona, Spain in 1991, and the "Doctor Ingeniero de Telecomunicación" degree from the "Universidad de Zaragoza" in 1997.

In 1991, he joined the "Antenas Microondas y Radar" group of the "Departamento de Teoría de la Señal y Comunicaciones" until 1992.

In 1992 he was employed in MIER COMUNICACIONES S.A. where he worked on the Solid State Power Amplifier design until 1993.

Since 1993, he has been an Assistant Professor and since 2001 Associate Professor at the "Departamento de Ingeniería Electrónica y Comunicaciones" at the "Universidad de Zaragoza." His research interests are in the area of linearization techniques of power amplifiers, power amplifier design, and mobile antenna systems.

Antonio Valdovinos (M'96) was born in Barbastro, Spain, in 1966. He received the Engineer of Telecommunications and Ph.D. degrees from the Universitat Politècnica de Catalunya (UPC), Spain, in 1990 and 1994, respectively.

In 1991 he joined, under a research grant, the Signal Theory and Communications Department, (UPC), where he was an Assistant Professor until 1995. In 1995 he joined the Centro Politécnico Superior, Universidad de Zaragoza (Spain) where he became an Associate Professor in 1996 and a Full Professor in 2003. At present his research interest lies in the area of wireless communications with special emphasis on Packet Radio Networks, Wireless Access Protocols, Radio Resources Management and QoS.